

*Physics**Physics Research Publications*

*Purdue University**Year 2007*

Suppressed decays of D-s(+) mesons to two pseudoscalar mesons

G. S. Adams, M. Anderson, J. P. Cummings, I. Danko, D. Hu, B. Moziak, J. Napolitano, Q. He, J. Insler, H. Muramatsu, C. S. Park, E. H. Thorndike, F. Yang, M. Artuso, S. Blusk, S. Khalil, J. Li, N. Menea, R. Mountain, S. Nisar, K. Randrianarivony, R. Sia, T. Skwarnicki, S. Stone, J. C. Wang, G. Bonvicini, D. Cinabro, M. Dubrovin, A. Lincoln, D. M. Asner, K. W. Edwards, P. Naik, R. A. Briere, T. Ferguson, G. Tatishvili, H. Vogel, M. E. Watkins, J. L. Rosner, N. E. Adam, J. P. Alexander, D. G. Cassel, J. E. Duboscq, R. Ehrlich, L. Fields, L. Gibbons, R. Gray, S. W. Gray, D. L. Hartill, B. K. Heltsley, D. Hertz, C. D. Jones, J. Kandaswamy, D. L. Kreinick, V. E. Kuznetsov, H. Mahlke-Kruger, D. Mohapatra, P. U. E. Onyisi, J. R. Patterson, D. Peterson, D. Riley, A. Ryd, A. J. Sadoff, X. Shi, S. Stroiney, W. M. Sun, T. Wilksen, S. B. Athar, R. Patel, J. Yelton, P. Rubin, B. I. Eisenstein, I. Karliner, N. Lowrey, M. Selen, E. J. White, J. Wiss, R. E. Mitchell, M. R. Shepherd, D. Besson, T. K. Pedlar, D. Cronin-Hennessy, K. Y. Gao, J. Hietala, Y. Kubota, T. Klein, B. W. Lang, R. Poling, A. W. Scott, P. Zweber, S. Dobbs, Z. Metreveli, K. K. Seth, A. Tomaradze, J. Ernst, K. M. Ecklund, H. Severini, W. Love, V. Savinov, A. Lopez, S. Mehrabyan, H. Mendez, J. Ramirez, J. Y. Ge, D. H. Miller, B. Sanghi, I. P. J. Shipsey, and B. Xin

This paper is posted at Purdue e-Pubs.

http://docs.lib.purdue.edu/physics_articles/859

Suppressed Decays of D_s^+ Mesons to Two Pseudoscalar Mesons

G. S. Adams,¹ M. Anderson,¹ J. P. Cummings,¹ I. Danko,¹ D. Hu,¹ B. Moziak,¹ J. Napolitano,¹ Q. He,² J. Insler,² H. Muramatsu,² C. S. Park,² E. H. Thorndike,² F. Yang,² M. Artuso,³ S. Blusk,³ S. Khalil,³ J. Li,³ N. Menea,³ R. Mountain,³ S. Nisar,³ K. Randrianarivony,³ R. Sia,³ T. Skwarnicki,³ S. Stone,³ J. C. Wang,³ G. Bonvicini,⁴ D. Cinabro,⁴ M. Dubrovin,⁴ A. Lincoln,⁴ D. M. Asner,⁵ K. W. Edwards,⁵ P. Naik,⁵ R. A. Briere,⁶ T. Ferguson,⁶ G. Tatishvili,⁶ H. Vogel,⁶ M. E. Watkins,⁶ J. L. Rosner,⁷ N. E. Adam,⁸ J. P. Alexander,⁸ D. G. Cassel,⁸ J. E. Duboscq,⁸ R. Ehrlich,⁸ L. Fields,⁸ L. Gibbons,⁸ R. Gray,⁸ S. W. Gray,⁸ D. L. Hartill,⁸ B. K. Heltsley,⁸ D. Hertz,⁸ C. D. Jones,⁸ J. Kandaswamy,⁸ D. L. Kreinick,⁸ V. E. Kuznetsov,⁸ H. Mahlke-Krüger,⁸ D. Mohapatra,⁸ P. U. E. Onyisi,⁸ J. R. Patterson,⁸ D. Peterson,⁸ D. Riley,⁸ A. Ryd,⁸ A. J. Sadoff,⁸ X. Shi,⁸ S. Stroiney,⁸ W. M. Sun,⁸ T. Wilksen,⁸ S. B. Athar,⁹ R. Patel,⁹ J. Yelton,⁹ P. Rubin,¹⁰ B. I. Eisenstein,¹¹ I. Karliner,¹¹ N. Lowrey,¹¹ M. Selen,¹¹ E. J. White,¹¹ J. Wiss,¹¹ R. E. Mitchell,¹² M. R. Shepherd,¹² D. Besson,¹³ T. K. Pedlar,¹⁴ D. Cronin-Hennessy,¹⁵ K. Y. Gao,¹⁵ J. Hietala,¹⁵ Y. Kubota,¹⁵ T. Klein,¹⁵ B. W. Lang,¹⁵ R. Poling,¹⁵ A. W. Scott,¹⁵ P. Zweber,¹⁵ S. Dobbs,¹⁶ Z. Metreveli,¹⁶ K. K. Seth,¹⁶ A. Tomaradze,¹⁶ J. Ernst,¹⁷ K. M. Ecklund,¹⁸ H. Severini,¹⁹ W. Love,²⁰ V. Savinov,²⁰ A. Lopez,²¹ S. Mehrabyan,²¹ H. Mendez,²¹ J. Ramirez,²¹ J. Y. Ge,²² D. H. Miller,²² B. Sanghi,²² I. P. J. Shipsey,²² and B. Xin²²

(CLEO Collaboration)

¹*Rensselaer Polytechnic Institute, Troy, New York 12180, USA*

²*University of Rochester, Rochester, New York 14627, USA*

³*Syracuse University, Syracuse, New York 13244, USA*

⁴*Wayne State University, Detroit, Michigan 48202, USA*

⁵*Carleton University, Ottawa, Ontario, Canada K1S 5B6*

⁶*Carnegie Mellon University, Pittsburgh, Pennsylvania 15213, USA*

⁷*Enrico Fermi Institute, University of Chicago, Chicago, Illinois 60637, USA*

⁸*Cornell University, Ithaca, New York 14853, USA*

⁹*University of Florida, Gainesville, Florida 32611, USA*

¹⁰*George Mason University, Fairfax, Virginia 22030, USA*

¹¹*University of Illinois, Urbana-Champaign, Illinois 61801, USA*

¹²*Indiana University, Bloomington, Indiana 47405, USA*

¹³*University of Kansas, Lawrence, Kansas 66045, USA*

¹⁴*Luther College, Decorah, Iowa 52101, USA*

¹⁵*University of Minnesota, Minneapolis, Minnesota 55455, USA*

¹⁶*Northwestern University, Evanston, Illinois 60208, USA*

¹⁷*State University of New York at Albany, Albany, New York 12222, USA*

¹⁸*State University of New York at Buffalo, Buffalo, New York 14260, USA*

¹⁹*University of Oklahoma, Norman, Oklahoma 73019, USA*

²⁰*University of Pittsburgh, Pittsburgh, Pennsylvania 15260, USA*

²¹*University of Puerto Rico, Mayaguez, Puerto Rico 00681*

²²*Purdue University, West Lafayette, Indiana 47907, USA*

(Received 31 July 2007; published 9 November 2007)

Using data collected near the $D_s^{*+}D_s^-$ peak production energy $E_{\text{cm}} = 4170$ MeV by the CLEO-c detector, we study the decays of D_s^+ mesons to two pseudoscalar mesons. We report on searches for the singly Cabibbo-suppressed D_s^+ decay modes $K^+\eta$, $K^+\eta'$, $\pi^+K_S^0$, $K^+\pi^0$, and the isospin-forbidden decay mode $D_s^+ \rightarrow \pi^+\pi^0$. We normalize with respect to the Cabibbo-favored D_s^+ modes $\pi^+\eta$, $\pi^+\eta'$, and $K^+K_S^0$, and obtain ratios of branching fractions: $\mathcal{B}(D_s^+ \rightarrow K^+\eta)/\mathcal{B}(D_s^+ \rightarrow \pi^+\eta) = (8.9 \pm 1.5 \pm 0.4)\%$, $\mathcal{B}(D_s^+ \rightarrow K^+\eta')/\mathcal{B}(D_s^+ \rightarrow \pi^+\eta') = (4.2 \pm 1.3 \pm 0.3)\%$, $\mathcal{B}(D_s^+ \rightarrow \pi^+K_S^0)/\mathcal{B}(D_s^+ \rightarrow K^+K_S^0) = (8.2 \pm 0.9 \pm 0.2)\%$, $\mathcal{B}(D_s^+ \rightarrow K^+\pi^0)/\mathcal{B}(D_s^+ \rightarrow K^+K_S^0) = (5.5 \pm 1.3 \pm 0.7)\%$, and $\mathcal{B}(D_s^+ \rightarrow \pi^+\pi^0)/\mathcal{B}(D_s^+ \rightarrow K^+K_S^0) < 4.1\%$ at 90% C.L., where the uncertainties are statistical and systematic, respectively.

DOI: 10.1103/PhysRevLett.99.191805

PACS numbers: 13.25.Ft

There are ten possible decays of D_s^+ mesons to a pair of mesons from the lowest-lying pseudoscalar meson nonet. The decay can be to either K^+ or π^+ , combined with any

of η , η' , π^0 , K^0 , or \bar{K}^0 (K_S^0 or K_L^0 for the final state). Measurements of the branching fractions of the complete set of decays test flavor topology and SU(3) predictions

[1]. The Cabibbo-favored, color-favored (external spectator) decays $D_s^+ \rightarrow \pi^+ \eta$ and $D_s^+ \rightarrow \pi^+ \eta'$ have been previously measured [2], as has the Cabibbo-favored, color-mixed (internal spectator) decay $D_s^+ \rightarrow K^+ K_S^0$ [2]. Here we present first observations of the singly Cabibbo-suppressed, color-favored decays $D_s^+ \rightarrow K^+ \eta$, $D_s^+ \rightarrow K^+ \eta'$, and $D_s^+ \rightarrow \pi^+ K_S^0$, and strong evidence [4.3 standard deviations (σ)] for the singly Cabibbo-suppressed, color-mixed decay $D_s^+ \rightarrow K^+ \pi^0$. (In this analysis, we have detected K_S^0 , but made no attempt to detect K_L^0 , nor have previous D_s^+ measurements.) We measure the ratio of the branching fraction of each singly Cabibbo-suppressed decay to that of the corresponding favored decay, expected to be, and found to be, of order $|V_{cd}/V_{cs}|^2 \approx 1/20$. The decay $D_s^+ \rightarrow \pi^+ \pi^0$ requires a change in isospin of 2 units and is thus “isospin forbidden” and expected to be substantially suppressed. Our search for this decay reveals no firm evidence for it, and we present an upper limit.

Data for this analysis were taken at the Cornell Electron Storage Ring (CESR) using the CLEO-c general-purpose solenoidal detector, which is described in detail elsewhere [3]. The charged particle tracking system covers a solid angle of 93% of 4π and consists of a small-radius, six-layer, low-mass, stereo wire drift chamber, concentric with, and surrounded by, a 47-layer cylindrical central drift chamber. The chambers operate in a 1.0 T magnetic field and achieve a momentum resolution of $\sim 0.6\%$ at $p = 1 \text{ GeV}/c$. We utilize two particle identification devices to separate charged kaons from pions: the central drift chamber, which provides measurements of ionization energy loss (dE/dx), and, surrounding this drift chamber, a cylindrical ring-imaging Cherenkov (RICH) detector, whose active solid angle is 80% of 4π . Detection of neutral pions and eta mesons relies on an electromagnetic calorimeter consisting of 7,784 cesium iodide crystals and covering 95% of 4π . The calorimeter achieves a photon energy resolution of 2.2% at $E_\gamma = 1 \text{ GeV}$ and 6% at 100 MeV.

We use 298 pb^{-1} of data produced in e^+e^- collisions at CESR near the center-of-mass energy $\sqrt{s} = 4170 \text{ MeV}$. Here the cross-section for the channel of interest, $D_s^{*+} D_s^-$ or $D_s^+ D_s^{*-}$, is $\sim 1 \text{ nb}$ [4]. We select events in which the D_s^* decays to $D_s + \gamma$ (94% branching fraction [2]). Other charm production totals $\sim 7 \text{ nb}$ [4], and the underlying light-quark “continuum” is about 12 nb. We reconstruct D_s^+ mesons in all two-body pseudoscalar decay channels. Throughout this Letter, charge conjugate modes are implicitly assumed, unless otherwise noted.

We use the reconstructed invariant mass of the D_s candidate, $M(D_s)$, and the mass recoiling against the D_s candidate, $M_{\text{recoil}}(D_s) \equiv \sqrt{(\sqrt{s} - E_{D_s})^2 - \vec{p}_{D_s}^2}$, as our primary kinematic variables to select a D_s candidate. Here \vec{p}_{D_s} is the momentum of the D_s candidate, $E_{D_s} = \sqrt{m_{D_s}^2 + \vec{p}_{D_s}^2}$, and m_{D_s} is the known D_s mass [2]. We make no requirements on the decay of the other D_s in the event.

There are two components in the recoil mass distribution, a peak around the D_s^* mass if the candidate is due to the primary D_s and a rectangular shaped distribution if the candidate is due to the secondary D_s from D_s^* decays. The edges of $M_{\text{recoil}}(D_s)$ from the secondary D_s are kinematically determined (as a function of \sqrt{s} and known masses), and at $\sqrt{s} = 4170 \text{ MeV}$, $\Delta M_{\text{recoil}}(D_s) \equiv M_{\text{recoil}}(D_s) - m_{D_s^*}$ is in the range $[-54, 57] \text{ MeV}$. Initial state radiation causes a tail on the high side, above 57 MeV. We select D_s candidates within the $-55 \text{ MeV} \leq \Delta M_{\text{recoil}}(D_s) < +55 \text{ MeV}$ range.

We also require a photon consistent with coming from $D_s^{*+} \rightarrow D_s^+ \gamma$ decay, by looking at the mass recoiling against the D_s candidate plus the γ system, $M_{\text{recoil}}(D_s + \gamma) \equiv \sqrt{(\sqrt{s} - E_{D_s} - E_\gamma)^2 - (\vec{p}_{D_s} + \vec{p}_\gamma)^2}$. For correct combinations, this recoil mass peaks at $m_{D_s^*}$, regardless of whether the candidate is due to a primary or a secondary D_s . We require $|M_{\text{recoil}}(D_s + \gamma) - m_{D_s^*}| < 20 \text{ MeV}$. Though there is a 25% efficiency loss from this requirement, it improves the signal to noise ratio, important for the suppressed modes.

Our standard final-state particle selection requirements are described in detail elsewhere [5]. Charged tracks produced in the D_s^+ decay are required to satisfy criteria based on the track fit quality, have momenta above $50 \text{ MeV}/c$, and angles with respect to the beam line, θ , satisfying $|\cos\theta| < 0.93$. They must also be consistent with coming from the interaction point in three dimensions. Pion and kaon candidates are required to have dE/dx measurements within 3 standard deviations (3σ) of the expected value. For tracks with momenta greater than $700 \text{ MeV}/c$, RICH information, if available, is combined with dE/dx . The efficiencies (95% or higher) and misidentification rates (a few percent) are determined with charged pions and kaons from hadronic D decays.

The K_S^0 candidates are selected from pairs of oppositely charged and vertex-constrained tracks having invariant mass within 12 MeV, or roughly 4.5σ , of the known K_S^0 mass. We identify π^0 candidates via $\pi^0 \rightarrow \gamma\gamma$, detecting the photons in the CsI calorimeter. To avoid having both photons in a region of poorer energy resolution, we require that at least one of the photons be in the “good barrel” region, $|\cos\theta_\gamma| < 0.8$. We require that the calorimeter clusters have a measured energy above 30 MeV, have a lateral distribution consistent with that from photons, and not be matched to any charged track. The invariant mass of the photon pair is required to be within 3σ ($\sigma \sim 6 \text{ MeV}$) of the known π^0 mass. A π^0 mass constraint is imposed when π^0 candidates are used in further reconstruction. We reconstruct η candidates in two decay modes. For the decay $\eta \rightarrow \gamma\gamma$, candidates are formed using a similar procedure as for π^0 except that $\sigma \sim 12 \text{ MeV}$. For $\eta \rightarrow \pi^+ \pi^- \pi^0$, we require that the invariant mass of the three pions be within 10 MeV of the known η mass. For this decay mode, we do not impose a mass constraint. We reconstruct η' candidates

in the decay mode $\eta' \rightarrow \pi^+ \pi^- \eta$. We require $|m_{\pi^+ \pi^- \eta} - m_{\eta'}| < 10$ MeV.

The D_s invariant mass distributions of the backgrounds to $D_s^+ \rightarrow K^+ K_S^0$ and $D_s^+ \rightarrow \pi^+ K_S^0$ are not smooth, but have bumps, caused by $D^{*+} D^{*-}$ events followed by $D^{*\pm} \rightarrow \pi^\pm D^0$ decays. The low-momentum π^\pm from D^0 decay, in combination with a particle from D^0 decay, can create a fake K_S^0 . To reduce the bump structure, which complicates fitting the background, we reject those $D_s^+ \rightarrow K^+ K_S^0$ and $D_s^+ \rightarrow \pi^+ K_S^0$ candidates that contain a π^+ or π^- with momentum below 100 MeV/c. To maintain cancellation of systematic errors, we also reject events with a K^\pm with momentum below 100 MeV/c. Further, we require that the K_S^0 has traveled a measurable distance from the interaction point before decaying, i.e., that the distance along the flight path, from interaction point to K_S^0 decay vertex, be greater than zero with a 3σ significance. After the low-momentum track veto and K_S^0 flight significance requirement are applied, no bump structures remain.

For the modes with η or η' , $\eta \rightarrow \gamma\gamma$, we reject the η candidate if either of the daughter photons is consistent with coming from $\pi^0 \rightarrow \gamma\gamma$ when paired with any other γ in the event. This veto reduces the background from fake $\gamma\gamma$ combination for η candidates, but causes a loss in efficiency of $\sim 30\%$.

The resulting $M(D_s)$ distributions for the Cabibbo-favored and Cabibbo-suppressed D_s modes are shown in Figs. 1 and 2, respectively. The points show the data and the lines are fits. We perform a binned maximum likelihood fit (2 MeV bins) to extract signal yields from the $M(D_s)$ distributions. For the signal, we use the sum of two Gaussians for the line shape. The signal shape parameters are determined by fits to $M(D_s)$ distributions obtained from a GEANT-based Monte Carlo (MC) simulation [6], with the proviso that the peak location of the primary Gaussian is allowed to shift in the fits to the Cabibbo-favored modes, and all other peak locations are shifted by the same amount. For $D_s^+ \rightarrow K^+ \pi^0$, where no appropriate Cabibbo-favored D_s decay exists, we have used the D^0 energy distribution of $D^0 \rightarrow K_S^0 \pi^0$, which indicates a peak shift of 5 MeV and a peak broadening of 10%. For the background, we use a second-degree polynomial function, allowing the overall scale, and the coefficient of the linear term relative to the constant term, to float in the fits to the data. We constrain the (very small) coefficient of the quadratic term relative to the constant term to the value given by MC simulation. We include as a systematic error the change in yield caused by varying the quadratic coefficient over a reasonable range, typically doubling the quadratic term coefficient, or setting it to zero. (For the favored modes, where the background is relatively smaller, we allow the coefficient of the quadratic term to float.) All fits have a $\chi^2/\text{d.o.f.} \approx 1.0$.

Results of the fits are shown in Table I. Also given in Table I is the detection efficiency for each mode, and, for

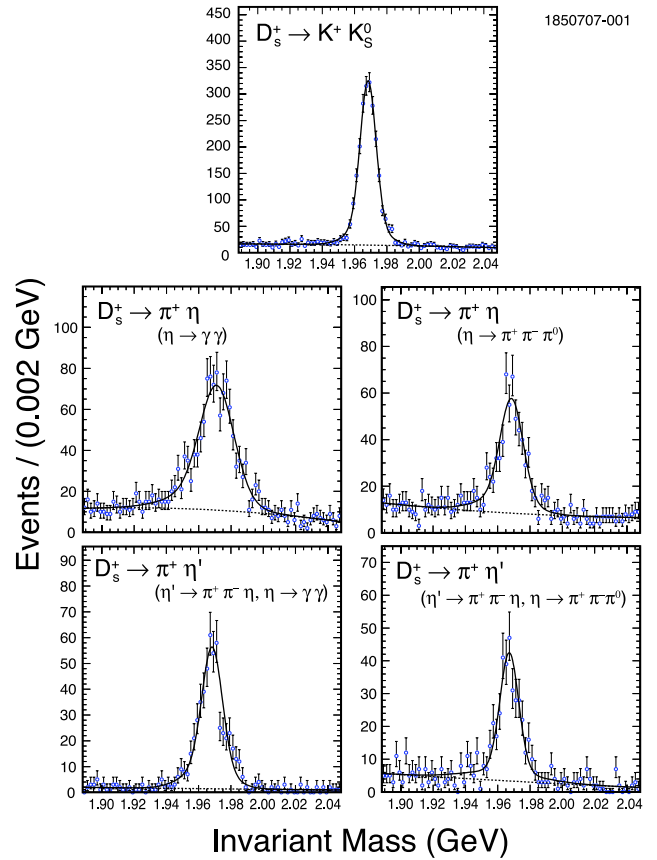


FIG. 1 (color online). $M(D_s)$ distributions for Cabibbo-favored D_s modes from data. The points are the data and the superimposed line is the fit (the dotted line is the fitted background) as described in the text.

the Cabibbo-suppressed modes, the statistical significance of the signal. We determine the significance by noting the decrease in the log likelihood when the fit is repeated with the signal constrained to zero. For $D_s^+ \rightarrow K^+ \pi^0$, the statistical significance is 4.3 standard deviations (σ), while for the modes using $\eta \rightarrow \gamma\gamma$, the statistical significance reaches or exceeds 5σ . The $\eta \rightarrow \pi^+ \pi^- \pi^0$ mode for $D_s^+ \rightarrow K^+ \eta$ confirms the signal, at 4.0σ , while for $D_s^+ \rightarrow K^+ \eta'$, due to the very large background of this mode, it gives no supporting evidence. For the $D_s^+ \rightarrow \pi^+ K_S^0$ mode, the statistical significance exceeds 10σ . For all Cabibbo-favored modes, very clear signals are found in the data.

We find no significant evidence for the isospin-forbidden decay $D_s^+ \rightarrow \pi^+ \pi^0$ and, therefore, set an upper limit on its rate. There is a large background from continuum events, and Monte Carlo studies indicate that tightening the requirement on $M_{\text{recoil}}(D_s)$ to ± 10 MeV should improve the upper limit. The invariant mass distribution with this requirement applied is shown in Fig. 2. We apply a sideband subtraction to the invariant mass distribution and obtain a yield of 17 ± 25 events. We interpret this result as implying a probability distribution for the true number of events N as a Gaussian, centered on 17, with width $\sigma = 25$, but

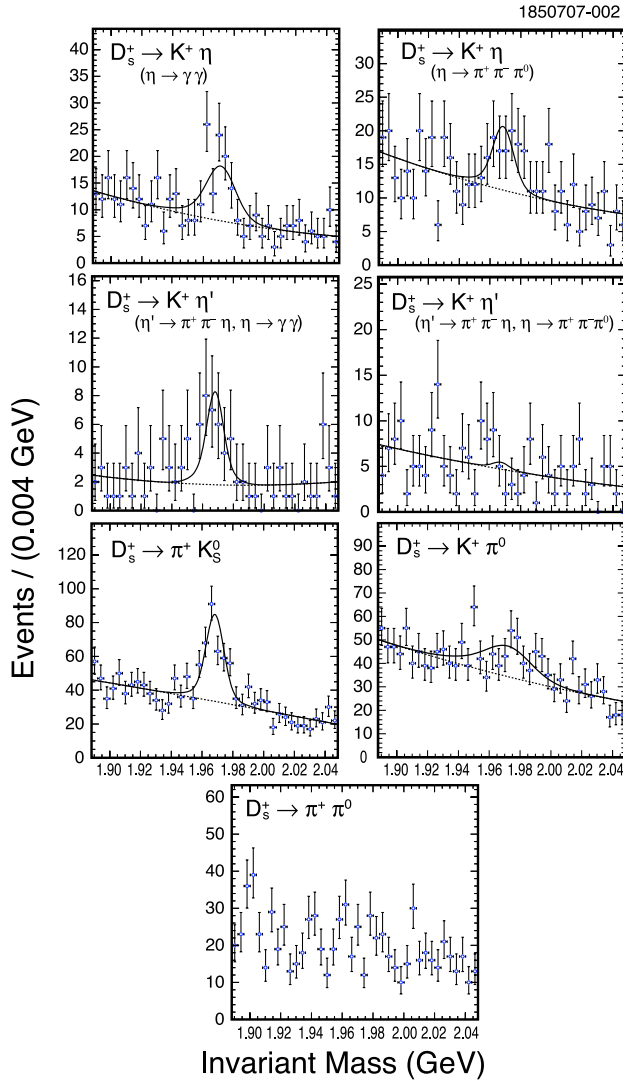


FIG. 2 (color online). $M(D_s)$ distributions for Cabibbo-suppressed D_s modes from data. The points are the data and the superimposed line is the fit (the dotted line is the fitted background) as described in the text. Also shown is the distribution for the isospin-forbidden decay $D_s^+ \rightarrow \pi^+ \pi^0$.

TABLE I. Observed yields from data and reconstruction efficiencies and their statistical uncertainties. For the Cabibbo-suppressed modes, the statistical significance of the signal is also given (see the text for details). The efficiencies include submode branching fractions [2], and have been corrected to include several known small differences between data and Monte Carlo simulation.

D_s Mode	Submode Decay	Yield	Significance (σ)	Efficiency (%)
$D_s^+ \rightarrow \pi^+ \eta$	$\eta \rightarrow \gamma\gamma$	908 ± 43		9.97 ± 0.05
$D_s^+ \rightarrow \pi^+ \eta$	$\eta \rightarrow \pi^+ \pi^- \pi^0$	512 ± 31		5.00 ± 0.03
$D_s^+ \rightarrow \pi^+ \eta'$	$\eta' \rightarrow \pi^+ \pi^- \eta, \eta \rightarrow \gamma\gamma$	509 ± 25		2.43 ± 0.02
$D_s^+ \rightarrow \pi^+ \eta'$	$\eta' \rightarrow \pi^+ \pi^- \eta, \eta \rightarrow \pi^+ \pi^- \pi^0$	344 ± 24		1.80 ± 0.01
$D_s^+ \rightarrow K^+ K_S^0$	$K_S^0 \rightarrow \pi^+ \pi^-$	2174 ± 52		26.13 ± 0.14
$D_s^+ \rightarrow \pi^+ K_S^0$	$K_S^0 \rightarrow \pi^+ \pi^-$	206 ± 22	11.1	29.93 ± 0.15
$D_s^+ \rightarrow K^+ \pi^0$	$\pi^0 \rightarrow \gamma\gamma$	141 ± 34	4.3	30.90 ± 0.14
$D_s^+ \rightarrow K^+ \eta$	$\eta \rightarrow \gamma\gamma$	68 ± 13	5.8	8.93 ± 0.05
$D_s^+ \rightarrow K^+ \eta$	$\eta \rightarrow \pi^+ \pi^- \pi^0$	45 ± 13	4.0	4.39 ± 0.03
$D_s^+ \rightarrow K^+ \eta'$	$\eta' \rightarrow \pi^+ \pi^- \eta, \eta \rightarrow \gamma\gamma$	25 ± 7	5.0	2.10 ± 0.02
$D_s^+ \rightarrow K^+ \eta'$	$\eta' \rightarrow \pi^+ \pi^- \eta, \eta \rightarrow \pi^+ \pi^- \pi^0$	3 ± 6	0.5	1.53 ± 0.01

truncated at zero, so the probability distribution vanishes for a negative true number of events. Ninety percent of the area of this distribution lies below 52 events, which we take as the 90% confidence level upper limit on the true number of events. We normalize this upper limit on yield to that for $D_s^+ \rightarrow K^+ K_S^0$, obtaining $\mathcal{B}(D_s^+ \rightarrow \pi^+ \pi^0)/\mathcal{B}(D_s^+ \rightarrow K^+ K_S^0) < 3.80 \times 10^{-2}$ (statistical only). Systematic errors, from the ratio of detection efficiencies, are $\pm 1.8\%$ for the K_S^0 detection, $\pm 4.2\%$ for the π^0 detection, 1.9% for the low-side tail on $M(D_s)$ caused by the π^0 , and other smaller errors, leading to a combined relative systematic error of $\pm 5.1\%$. We conservatively increase the upper limit by 1.28 times the combined systematic errors, giving an upper limit, including systematic errors, of 4.1×10^{-2} .

In principle, nonresonant D_s decay could enter into our signal modes with the same final particles. For example, nonresonant $D_s^+ \rightarrow \pi^+(\pi^+ \pi^- \pi^0)$ could appear in the $D_s^+ \rightarrow \pi^+ \eta, \eta \rightarrow \pi^+ \pi^- \pi^0$ mode. To understand the background from nonresonant D_s decay, we look at $M(D_s)$ distributions in the sideband region of the intermediate resonance (η, η' , or K_S^0) invariant mass. These studies show that the nonresonant modes produce negligible contributions to our signal modes.

For the modes with η or η' ($\eta' \rightarrow \pi^+ \pi^- \eta$) in the final state, we reconstruct these modes with η decaying to $\gamma\gamma$ and to $\pi^+ \pi^- \pi^0$. For Cabibbo-favored modes, we combine the two fit yields from the different η decay modes according to the fit yield fractional error. The weighting factors for both $D_s^+ \rightarrow \pi^+ \eta$ and $D_s^+ \rightarrow \pi^+ \eta'$ are 0.65 for $\eta \rightarrow \gamma\gamma$ and 0.35 for $\eta \rightarrow \pi^+ \pi^- \pi^0$. We apply the same weighting factors to the corresponding Cabibbo-suppressed modes ($D_s^+ \rightarrow K^+ \eta$ and $D_s^+ \rightarrow K^+ \eta'$). Doing so guarantees cancellation of systematic errors between Cabibbo-favored and Cabibbo-suppressed modes. It also avoids a possible bias that could come from using the errors on the Cabibbo-suppressed modes to determine the weighting factors for them.

Ratios of branching fractions are computed for each of the Cabibbo-suppressed modes and are presented in

TABLE II. Ratios of branching fractions of Cabibbo-suppressed modes to corresponding Cabibbo-favored modes. Uncertainties are statistical and systematic, respectively.

Mode	$\mathcal{B}_S/\mathcal{B}_F(10^{-2})$
$\mathcal{B}(D_s^+ \rightarrow K^+ \eta)/\mathcal{B}(D_s^+ \rightarrow \pi^+ \eta)$	$8.9 \pm 1.5 \pm 0.4$
$\mathcal{B}(D_s^+ \rightarrow K^+ \eta')/\mathcal{B}(D_s^+ \rightarrow \pi^+ \eta')$	$4.2 \pm 1.3 \pm 0.3$
$\mathcal{B}(D_s^+ \rightarrow \pi^+ K_S^0)/\mathcal{B}(D_s^+ \rightarrow K^+ K_S^0)$	$8.2 \pm 0.9 \pm 0.2$
$\mathcal{B}(D_s^+ \rightarrow K^+ \pi^0)/\mathcal{B}(D_s^+ \rightarrow K^+ K_S^0)$	$5.5 \pm 1.3 \pm 0.7$
$\mathcal{B}(D_s^+ \rightarrow \pi^+ \pi^0)/\mathcal{B}(D_s^+ \rightarrow K^+ K_S^0)$	<4.1 (90% C.L.)

Table II. They are normalized with respect to the corresponding Cabibbo-favored modes. We use the $D_s^+ \rightarrow K^+ K_S^0$ mode to normalize the $D_s^+ \rightarrow K^+ \pi^0$ mode. The upper limit for the unobserved mode $D_s^+ \rightarrow \pi^+ \pi^0$, normalized with respect to $D_s^+ \rightarrow K^+ K_S^0$, is also shown in Table II.

We have considered several sources of systematic uncertainty. Finite MC statistics in determining reconstruction efficiencies introduces uncertainties at the level of less than 1%. The uncertainty associated with the efficiency for finding a track is 0.3%; an additional 0.6% systematic uncertainty for each kaon track is added. The relative systematic uncertainties for π^0 and K_S^0 efficiencies are 4.2% and 1.8%, respectively. The systematic uncertainty for η efficiencies cancels in all ratios. Uncertainties in the charged pion and kaon identification efficiencies are 0.3% per pion and 1.3% per kaon [5]. The systematic uncertainties from the K_S^0 flight significance requirement and the low-momentum track veto are 0.5% and 0.3%, respectively. The signal shape parameters are taken from MC simulation and have uncertainties related to possible flaws in simulation. For all ratios except $\mathcal{B}(D_s^+ \rightarrow K^+ \pi^0)/\mathcal{B}(D_s^+ \rightarrow K^+ K_S^0)$, numerator and denominator are topologically similar, and any defects in Monte Carlo calculations will cancel in the ratio. For $D_s^+ \rightarrow K^+ \pi^0$, we have determined the shift in peak location and change in peak width from $D^0 \rightarrow K_S^0 \pi^0$. We conservatively take half of the 5 MeV peak shift, and half of the 10% increase in peak width, as the systematic error, thereby obtaining $\pm 4.9\%$. For the suppressed modes, the background quadratic term is also taken from MC simulation. We vary that term over a reasonable range, finding a systematic error of 2.4% to 10.6%, depending on mode.

In calculating the relative systematic uncertainties for the measured ratio of Cabibbo-suppressed mode branching fractions to Cabibbo-favored mode branching fractions ($\mathcal{B}_{\text{Suppressed}}/\mathcal{B}_{\text{Favored}}$), cancellation of uncertainties has been taken into account. The systematic uncertainties that do not cancel in the ratios are added in quadrature to obtain the total systematic uncertainties shown as the second error in Table II. For the upper limit in Table II, the systematic uncertainties have been included as previously described. Systematic uncertainties for all measured ratios are at most half the statistical uncertainties.

TABLE III. Measured CP asymmetries in Cabibbo-suppressed decay modes. Only statistical uncertainties are included. Systematic errors are negligible by comparison.

Mode	$(\mathcal{B}_+ - \mathcal{B}_-)/(\mathcal{B}_+ + \mathcal{B}_-)$ (%)
$\mathcal{A}(D_s^+ \rightarrow K^+ \eta)$	-20 ± 18
$\mathcal{A}(D_s^+ \rightarrow K^+ \eta')$	-17 ± 37
$\mathcal{A}(D_s^+ \rightarrow \pi^+ K_S^0)$	27 ± 11
$\mathcal{A}(D_s^+ \rightarrow K^+ \pi^0)$	2 ± 29

The standard model predicts that direct CP violation in D decays, e.g., a difference in the branching fractions for $D_s^+ \rightarrow K^+ \eta$ and $D_s^- \rightarrow K^- \eta$, will be vanishingly small. As a search for evidence of non-standard-model physics, we have therefore measured the CP asymmetries $\mathcal{A} \equiv (\mathcal{B}_+ - \mathcal{B}_-)/(\mathcal{B}_+ + \mathcal{B}_-)$ for the four Cabibbo-suppressed D_s decay modes we are studying. Results are given in Table III. Errors shown are statistical. The systematic errors, from the differences in efficiency for detecting K^+ vs. K^- and π^+ vs. π^- , are $<2.0\%$, negligible by comparison. All asymmetries are consistent with zero.

In summary, we report first observations of four Cabibbo-suppressed decays of D_s mesons and measure the ratio of their branching fractions to the corresponding Cabibbo-favored modes. We find those ratios to be of order $|V_{cd}/V_{cs}|^2 \approx 1/20$ in agreement with naive expectations. We report a first upper limit on the isospin-forbidden decay $D_s^+ \rightarrow \pi^+ \pi^0$. The CP asymmetries for the four Cabibbo-suppressed decays are consistent with zero, as predicted by the standard model.

We gratefully acknowledge the effort of the CESR staff in providing us with excellent luminosity and running conditions. This work was supported by the A.P. Sloan Foundation, the National Science Foundation, the U.S. Department of Energy, and the Natural Sciences and Engineering Research Council of Canada.

-
- [1] C. W. Chiang, Z. Luo, and J. L. Rosner, Phys. Rev. D **67**, 014001 (2003).
 - [2] W.-M. Yao *et al.* (Particle Data Group), J. Phys. G **33**, 1 (2006).
 - [3] Y. Kubota *et al.*, Nucl. Instrum. Methods Phys. Res., Sect. A **320**, 66 (1992); D. Peterson *et al.*, Nucl. Instrum. Methods Phys. Res., Sect. A **478**, 142 (2002); M. Artuso *et al.*, Nucl. Instrum. Methods Phys. Res., Sect. A **554**, 147 (2005).
 - [4] R. Poling, in *Proceedings of 4th Flavor Physics and CP Violation Conference (FPCP 2006), Vancouver, British Columbia, Canada, 2006*, econf C060409, 005 (2006).
 - [5] Q. He *et al.* (CLEO Collaboration), Phys. Rev. Lett. **95**, 121801 (2005).
 - [6] R. Brun *et al.*, GEANT 3.21, CERN Program Library Long Writeup Report No. W5013 (unpublished).